An Efficient Method for Complex Antenna Design Based on a Self Adaptive Surrogate Model Assisted Optimization Technique

Bo Liu *Senior Member, IEEE*, Mobayode O. Akinsolu *Member, IEEE*, Chaoyun Song *Member, IEEE*, Qiang Hua *Student Member, IEEE*, Peter Excell *Life Senior Member, IEEE*, Qian Xu, Yi Huang *Senior Member, IEEE*, Muhammad Ali Imran *Senior Member, IEEE*,

***Abstract*—Surrogate models are widely used in antenna design for optimization efficiency improvement. Currently, the targeted antennas often have a small number of design variables and specifications, and the surrogate model training time is short. However, modern antennas become increasingly complex which need much more design variables and specifications, making the training time become a new bottleneck, i.e., in some cases even longer than electromagnetic (EM) simulation time. Therefore, a new method, called training cost reduced surrogate model-assisted hybrid differential evolution for complex antenna optimization (TR-SADEA) is presented in this paper. The key innovations include: (1) A self-adaptive Gaussian Process surrogate modeling method with a significantly reduced training time whilst mostly maintaining the antenna performance prediction accuracy, and (2) A new hybrid surrogate model-assisted antenna optimization framework which reduces the training time and increases the convergence speed. An indoor base station antenna with 2G to 5G cellular bands (45 design variables, 12 specifications) and a 5G outdoor base station antenna (23 design variables, 18 specifications) are used to demonstrate TR-SADEA. Experimental results show that more than 90% of the training time and about 20% iterations (simulations and surrogate modeling) are reduced compared to a state-of-the-art method while obtaining high antenna performance.**

***Index Terms*—5G base station antenna; Antenna design; Complex antenna; Computationally expensive optimization; Differential evolution; Gaussian process; Radial basis function; Surrogate model**

I. Introduction

Antenna design optimization has been investigated for two decades. To find the optimal design satisfying the antenna specifications, existing optimization techniques mainly include local optimization-driven methods [1], [2] and global optimization-driven methods [3], [4], [5]. Compared with local optimizers, global optimizers have the advantages of optimization capability, not requiring an initial design and robustness [6], [7]. Among global optimizers, arguably, differential evolution (DE) [8] and particle swarm optimization (PSO) [9] tend to play a leading role [3], [6].

However, full-wave electromagnetic (EM) simulation, which is often necessary in antenna optimization [10], is computationally expensive. Global optimization techniques often need a large number of such simulations, which could be a few thousands or more for many antenna cases [5]. Thus, obtaining optimal designs in a reasonable optimization time becomes a challenge. Therefore, surrogate models, which are constructed by machine learning techniques, are introduced to replace computationally expensive EM simulations so as to significantly reduce the computational cost [1], [5], [11]. Prediction uncertainty is unavoidable when employing surrogate models and a poor surrogate model may fail the optimization. The method to find an appropriate trade-off between the surrogate model quality and the efficiency (i.e., the number of necessary EM simulations) is the key issue, which is called model management [12]. Using different model management methods, various efficient antenna optimization approaches are produced.

The surrogate model-assisted differential evolution for antenna optimization (SADEA) method [5] is one of the state-of-the-art approaches. Comparisons using practical antennas show that SADEA (first generation) can satisfy design specifications that DE and PSO are not able to and has up to an order of magnitude speed improvement compared to them [5], [13]. The surrogate modeling of SADEA is then improved in [14]. Multi-fidelity and parallel SADEA are then developed [14], [15], [16]. The new search and model management methods in parallel SADEA obtain another 1.5 to 2 times speed improvement even without considering the time saved by parallel EM simulations [15], [16].

Most surrogate model-assisted antenna optimization methods, including the SADEA series, employ Gaussian process (GP) surrogate model due to its strong learning ability [10]. At present, the targeted antennas often have around 10 design variables and the number of specifications is often not more than a few (e.g., S_{11}, gain, axial ratio). For these cases, the training time of a reliable GP model is often within a few seconds using a normal desktop workstation (e.g., intel i7 3.0 GHz CPU), which is negligible compared to an EM

B. Liu and M. Imran are with School of Engineering, University of Glasgow, Scotland. (e-mail: Bo.Liu@glasgow.ac.uk, Muhammad.Imran@glasgow.ac.uk).

M. O. Akinsolu and P. Excell are with School of Art and Science, Wrexham Glyndwr University, U.K. (e-mail: m.o.akinsolu@ieee.org, p.excell@glyndwr.ac.uk).

C. Song is with School of Engineering, Heriot-Watt University, Scotland. (e-mail: cs395@hw.ac.uk).

Q. Hua and Y. Huang are with Department of Electrical Engineering, University of Liverpool, UK. (e-mail: Qiang.Hua@liverpool.ac.uk, Yi.Huang@liverpool.ac.uk)

Q. Xu is with College of Electronic and Information Engineering, Nanjing University of Aeronautics and Astronautics, China (e-mail: emxu@foxmail.com).

Corresponding authors: Bo Liu (algorithm), Yi Huang (design)

simulation. However, modern antennas become increasingly complex [17], [18], [19]. They often have several tens of critical design variables and quite a few design specifications. Without considering the challenge in terms of optimization ability, the large number of design variables and specifications [20], [21] makes the surrogate modeling time become another bottleneck, which is worse than EM simulations in many occasions. (Examples are shown in Section IV.)

The total training time of GP models in the optimization process can be estimated as $T_{GP} \times N_{specs} \times N_{pop} \times N_{it}$, where T_{GP} is the training time of each GP model, N_{specs} is the number of specifications, N_{pop} is the number of candidate designs in a population, and N_{it} is the number of iterations in antenna optimization. For complex antennas, besides the direct impact of the much larger N_{specs}, the large number of design variables (d) has the following effects: T_{GP} becomes much larger because the training time of GP grows cubically with the number of training data points [22]. To obtain a reliable surrogate model, a certain number of training data points growing with d are needed around a candidate design (e.g., at least $4 \times d$ from [5]). To maintain the exploration ability, N_{pop} is also highly affected by d (e.g., $2.5 \times d$ to $5 \times d$ from [5], [6]). Because of the large d, more iterations are necessary to reach the optimal design, and N_{it} also increases. This makes the GP modeling time become the bottleneck, which can be several weeks in standard SADEA when using a normal desktop workstation [23].

Owing to this, a new algorithm, called training cost reduced surrogate model-assisted hybrid differential evolution for complex antenna optimization (TR-SADEA) is proposed. To the best of our knowledge, TR-SADEA is the first method focusing on complex antennas, targeting at reducing the induced very long surrogate modeling time to an acceptable level while maintaining high antenna performance. The key innovations include: (1) A self-adaptive GP modeling method with a significantly reduced training cost while mostly maintaining the antenna performance prediction accuracy; and (2) A new hybrid surrogate model-assisted antenna optimization framework introducing a computationally cheap radial basis function (RBF) model-assisted local optimization stage into SADEA. Besides replacing many GP modeling, it further increases the convergence speed. Note that the innovations are compatible with many existing methods.

The remainder of the paper is organized as follows: Section II presents the basic techniques. Section III elaborates on the TR-SADEA method. Section IV presents the performance of TR-SADEA using an indoor base station antenna with 2G to 5G cellular bands and a 5G outdoor base station antenna. The concluding remarks are provided in Section V.

II. Basic Techniques

A. Gaussian Process

GP [24], [25] is arguably the most widely used machine learning method in antenna design optimization. Given a set of observations $x = (x^1, \ldots, x^n)$ and $y = (y^1, \ldots, y^n)$, GP predicts a function value $y(x)$ at some design point x by modeling $y(x)$ as a Gaussian distributed stochastic variable with mean μ and variance σ^2. If the function is continuous, the function values of two points x^i and x^j should be close if they are highly correlated. In this work, we use the Gaussian correlation function to describe the correlation between two variables:

$$\begin{aligned} &Corr(x_i, x_j) = exp(-\textstyle\sum_{l=1}^{d} \theta_l |x_i^l - x_j^l|^{p_l}) \\ &\theta_l > 0, 1 \le p_l \le 2 \end{aligned} \tag{1}$$

where d is the dimension of x and θ_l is the correlation parameter which determines how fast the correlation decreases when x_i moves in the l direction. The smoothness of the function is related to p_l with respect to x^l. To determine the parameters θ_l and p_l, the likelihood function that $y = y^i$ at $x = x^i (i = 1, \ldots, n)$ is maximized. The function value $y(x^*)$ at a new point x^* can be predicted as:

$$\hat{y}(x^*) = \hat{\mu} + r^T R^{-1}(y - I\hat{\mu}) \tag{2}$$

where

$$R_{i,j} = Corr(x_i, x_j), i, j = 1, 2, \ldots, n \tag{3}$$

$$r = [Corr(x^*, x_1), Corr(x^*, x_2), \ldots, Corr(x^*, x_n)] \tag{4}$$

$$\hat{\mu} = (I^T R^{-1} I)^{-1} I^T R^{-1} y \tag{5}$$

The mean square error value of the prediction uncertainty is:

$$\hat{s}^2(x^*) = \hat{\sigma}^2[I - r^T R^{-1} r + (I - r^T R^{-1} r)^2 (I^T R^{-1} I)^{-1}] \tag{6}$$

where

$$\hat{\sigma^2} = (y - I\hat{\mu})^T R^{-1}(y - I\hat{\mu}) n^{-1} \tag{7}$$

The lower confidence bound (LCB) method [22], [26] is used. Given the predictive distribution $N(\hat{y}(x), \hat{s}^2(x))$ for $y(x)$, a lower confidence bound prescreening of $y(x)$ can be defined as:

$$y_{lcb}(x) = \hat{y}(x) - \omega \hat{s}(x) \tag{8}$$

where $\omega \in [0, 3]$ is a constant, which is often set to 2 to balance the exploration and exploitation ability [22]. The ooDACE toolbox [27] is used for implementing GP.

The computational complexity of GP modeling is $O(N_G n^3 d)$ [22], where N_G is the number of iterations spent in hyper-parameter optimization and n is the number of training data points. The most critical factor is n, which is affected by d to construct a reliable GP model (Section I). Therefore, the computational cost of GP modeling can be very high when the number of design variables is large [28], [29].

B. Radial Basis Function

RBF [30] is another popular machine learning method for surrogate modeling. Its learning ability is not as high as GP but its training is computationally much cheaper [31]. For several complex antenna test cases, the RBF modeling time for a candidate design is often less than 30 seconds using a normal desktop workstation even if 1000 training data points are used. Given a set of observations $x = (x^1, \ldots, x^n)$ and

$y = (y^1, \ldots, y^n)$, RBF predicts the function value $y(x^*)$ at a new point x^* as:

$$\hat{y}(x^*) = \sum_{i=1}^{n} \lambda_i \phi(||x^* - x^i||) + p(x) \tag{9}$$

where λ are the coefficients, $p(x)$ is a linear polynomial with d variables and $p(x) = \sum_{j=1}^{d+1} b_j x_j$. ϕ is a basis function, which is monotonic. In this implementation, the cubic form, $\phi(x) = x^3$ is used. To fit this model, the hyperparameters $\lambda = [\lambda_1, \lambda_2, \ldots, \lambda_n]^T$ and $B = [b_1, b_2, \ldots, b_{d+1}]^T$ can be calculated by solving:

$$\begin{bmatrix} \Phi & P_r \\ P_r^T & 0_{(d+1)\times(d+1)} \end{bmatrix} \begin{bmatrix} \lambda \\ B \end{bmatrix} = \begin{bmatrix} y \\ 0_{d+1} \end{bmatrix} \tag{10}$$

where $\Phi \in R^{n\times n}$ and $\Phi_{ij} = \phi(||x^i - x^j||)$, $i, j = 1, 2, \ldots, n$. $P_r \in R^{n\times(d+1)}$ and the i^{th} row of P_r is $[1, x^i]$.

C. The DE Algorithm

The DE algorithm [8] is adopted as the search engine in TR-SADEA. Suppose that P is a population. Let $x = (x_1, \ldots, x_d) \in R^d$ be an individual solution in P. To generate a child solution $u = (u_1, \ldots, u_d)$ for x, a donor vector is first produced by mutation (the DE/current-to-best/1 strategy is used in this paper):

$$v^i = x^i + F \cdot (x^{best} - x^i) + F \cdot (x^{r_1} - x^{r_2}) \tag{11}$$

where x^i is the i^{th} vector in the current population and x^{best} is the best candidate in the current population P, x^{r_1} and x^{r_2} are mutually exclusive solutions randomly selected from P (the current population); v^i is the i^{th} mutant vector in the population after mutation; $F \in (0, 2]$ is a control parameter, often called the scaling factor.

Then the following crossover operator is applied to produce the child u:

1 Randomly select a variable index $j_{rand} \in \{1, \ldots, d\}$,

2 For each $j = 1$ to d, generate a uniformly distributed random number $rand$ from $(0, 1)$ and set:

$$u_j = \begin{cases} v_j, & \text{if } (rand \le CR) | j = j_{rand} \\ x_j, & \text{otherwise} \end{cases} \tag{12}$$

where $CR \in [0, 1]$ is a constant called the crossover rate.

III. The TR-SADEA Method

A. The Algorithm Framework

As said in Section I, complex antennas often involve many design variables and specifications. Long training time for such problems is a well-known challenge for GP modeling in the computational intelligence field [28], [31], [32]. Existing solutions mainly include finding substitutions from other machine learning methods [28], [31] and simplifying hyperparameters in the GP training process [32]. They are successful methods, but the degradation of model quality is unavoidable and our initial investigation found that these solutions are not fit for antenna design landscape characteristics. Note that antenna design optimization is challenging and popular (surrogate model-assisted) optimization algorithms that are successful for various mathematical benchmark problems are not successful for antenna optimization test cases [13].

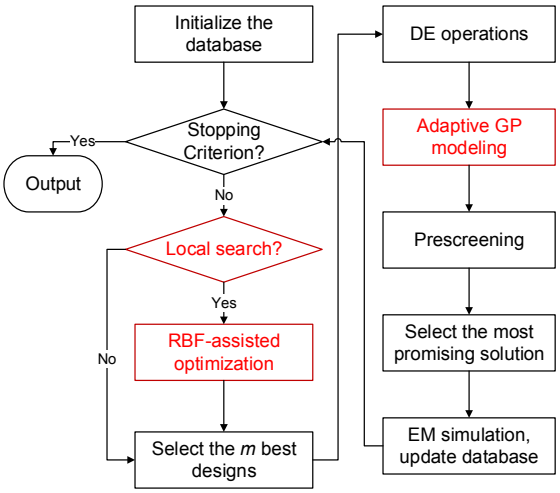

Figure 1. Flow diagram of TR-SADEA

To highly reduce the GP modeling time while maintaining the design solution quality, two novel methods are proposed. In the following, the general framework of TR-SADEA is first provided and details of the two new methods are then described in Section III (B) and (C).

The TR-SADEA framework is shown in Fig. 1, which works as follows.

Step 1: Sample α (often a small number of) candidate designs from the design space $[LB, UB]^d$ (LB and UB are the lower and upper bounds of design variables, respectively) using Latin Hypercube Sampling (LHS) [33], evaluate the objective function values of all these solutions using EM simulations and let them form the initial database.

Step 2: If a preset stopping criterion is met (e.g., the computing budget is exhausted), output the best solution from the database; otherwise go to Step 3.

Step 3: Judge whether local optimization should be used or not. If yes, carry out the RBF-assisted local optimization with the current best design as the starting point. Update the current best design when necessary.

Step 4: Select the m best designs from the database to form a population P.

Step 5: Apply the DE mutation (11) and crossover (12) operations to P to generate m new child solutions.

Step 6: Build N_c GP models self-adaptively.

Step 7: Estimate the m child solutions generated in Step 5 using the GP models in Step 6 and the lower confidence bound method (8).

Step 8: Evaluate the EM simulation model at the predicted best child candidate design from Step 7. Add this candidate design and its performance values to the database. Go back to Step 2.

It can be seen that some model management operators are

borrowed from standard SADEA [5]. The model management method of SADEA is different from the traditional method of first constructing a high-quality surrogate model and performing optimization based on it. The resulted benefits are much higher efficiency and scalability. Details are in [5], [34]. The two novel methods, the self-adaptive GP modeling (Step 6) and the RBF-assisted local optimization (Step 3) targeting at addressing the challenge in long surrogate modeling time are shown as red blocks in Fig. 1 and are detailed below. Note that they are also compatible with other antenna optimization methods.

B. The Self-adaptive GP Modeling Method

Recall in Section I that $N_{specs} \times N_{pop}$ (see definitions in Section I) GP models need to be built in each iteration of the optimization, costing a long time. In TR-SADEA, our central idea is to build much fewer than N_{pop} GP models for each specification and many candidate designs share the same GP model when possible. It is clear that much more training time can be saved but the prediction accuracy becomes the main issue. Two questions are introduced: (1) What is the appropriate number of GP models which maintains the prediction accuracy and saves the training time as much as possible? (2) How to select the training data points for a GP model predicting a group of (instead of a single) candidate designs? To address the above questions, a new self-adaptive GP modeling method is proposed, which works as follows.

Step 1: Cluster the population P waiting to be predicted into N_c clusters by the K-means method [35]. N_c starts from 1.

Step 2: For each member in each cluster, select the nearest (Euclidean distance) $4 \times d$ simulated candidate designs as its training data points. Collect the training data points for all the members in the cluster to construct the preliminary training data set for each cluster ($T_{cp}\{cluster_i\}$). After this step, T_{cp} has N_c elements ($T_{cp}\{cluster_1\}$ to $T_{cp}\{cluster_{N_c}\}$).

Step 3: For each element in T_{cp} ($T_{cp}\{cluster_i\}$), rank the set based on number of appearance and distance to the cluster center. Select the top $4 \times d$ points of $T_{cp}\{cluster_i\}$ to be the final training data set $T_{cf}\{cluster_i\}$. After this step, T_{cf} has N_c elements.

Step 4: For each element in T_{cf} ($T_{cf}\{cluster_i\}$), calculate the average Euclidean distance between the training data points and the cluster centroid ($dist_t$), and the average Euclidean distance between individuals in P for the same cluster and the cluster centroid ($dist_p$).

Step 5: If for all the clusters, $\frac{dist_p}{dist_t} \leq 1$, use the N_c clusters and train N_c GP models by T_{cf}. Otherwise, increase N_c by 1 and go back to Step 1.

Note that the above ranking method is used when the number of simulated designs is larger than $4 \times d$; Otherwise; all of the simulated designs are used to construct the N_c GP models. It can be seen that the number of GP models (i.e., the number of clusters) is determined self-adaptively. Fig. 2 shows two kinds of data distribution. In Fig. 2(a), the training data points are inside the data points to be predicted, and

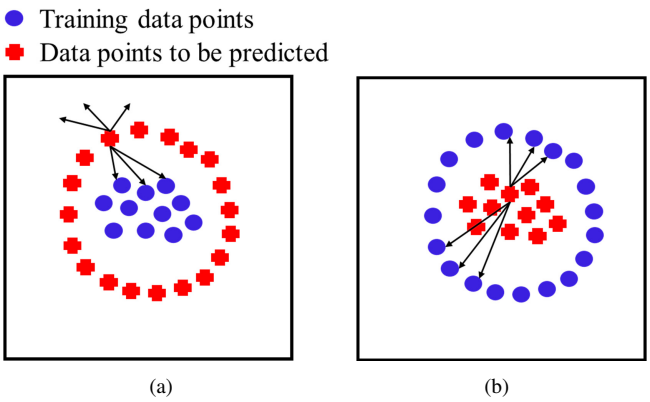

Figure 2. Two kinds of distributions of training data points and data points to be predicted.

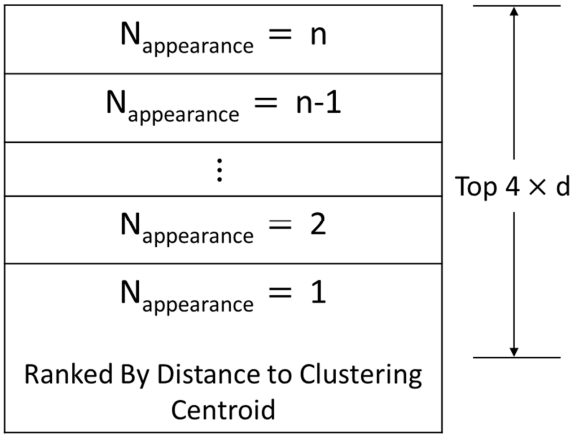

Figure 3. An illustrative figure of training data points selection

in Fig. 2(b), it is the opposite. It is unlikely that (a) can obtain a good prediction result because for the data points to be predicted, the correlations with training data points (according to (1)) from some directions are not available. In contrast, the prediction accuracy of (b) is better because the correlations with training data points are available from all directions. Therefore, the criterion is that the training data set must at least encompass the data that needs to be predicted. We describe this by $\frac{dist_p}{dist_t} \leq 1$. The threshold is selected to be 1, which means that the two sets are approximately in the same position. Experiments using various antennas show that using the threshold of 1 has a high rate of successful design optimization. By decreasing this threshold, the data that needs to be predicted are enveloped to a larger extent but N_c will increase, costing more computing overhead.

Regarding the method to select the training data points for a GP model predicting a group of candidate designs, the ranking method in Step 3 is as follows. Clearly, selecting the top $4 \times d$ training data points instead of using all of the data in $T_{cp}\{cluster_i\}$ is necessary because of the GP modeling time. Thus, which points should be used from $T_{cp}\{cluster_i\}$ is important. The first ranking criterion is the number of appearances in T_{cp}, which shows that a training data point is useful for a corresponding number of points to be predicted, playing the main role. For the training data points which only

appear for once in $T_{cp}\{cluster_i\}$ (i.e., it is only useful for the prediction of a single candidate solution), the nearer to clustering centroid, the more information it provides, which is the second ranking criterion. An illustrative figure is Fig. 3.

C. The RBF-assisted Local Optimization

At the beginning period of antenna optimization, most of the candidate designs in P (the population of candidate designs, Section III (A)) are far from optimal. Therefore, finding improved designs in this period is much easier than the later period, when candidate designs in P are of reasonably good quality. Owing to this, a surrogate model with reduced prediction ability compared to GP is useful in this period. In TR-SADEA, RBF models are built. The selected optimizer is sequential quadratic programming (SQP) [36], which is a popular local optimization method, to compensate with the DE search. The starting point of this local optimization is the current best design, and this local optimization aims to improve it.

The RBF-assisted local optimization introduces two benefits: (1) The GP modeling used at the beginning period of optimization is replaced by RBF modeling. The RBF model training time is often within a few seconds, which is negligible. (2) In Step 4 of the TR-SADEA framework, DE/current-to-best/1 (11) mutation strategy is used. Therefore, the pattern of an improved current best design by this local optimization can be transferred to all the child solutions through DE/current-to-best/1, which improves the convergence speed of the whole algorithm, indicating a fewer number of overall EM simulations and GP modeling.

The RBF-assisted local optimization (Step 3 of the TR-SADEA framework) works as follows. SQP is implemented by MATLAB Optimization Toolbox.

- **Step 1:** Select $10\times d$ nearest (Euclidean distance) candidate designs around the current best design from the database. If the number of simulated designs is fewer than $10 \times d$, select all of them.
- **Step 2:** Construct an RBF model using the selected training data points.
- **Step 3:** Carry out SQP optimization using the RBF model to obtain a local optimal design x_o. No EM simulations is used in this step.
- **Step 4:** If the RBF predicted objective function value of x_o is better than the real objective function value using EM response of the current best design, carry out an EM simulation to x_o. Add this design to the database.
- **Step 5:** If the real objective function value using EM response of x_o is better than that of the current best design, update the current best design.

Our initial investigation shows that this RBF-assisted local optimization is effective at the beginning period, but its effectiveness decreases with the progress of optimization. The reason was mentioned before. It is clear that running it in the whole TR-SADEA will waste EM simulations. Hence, the rate of using this RBF-assisted local optimization is calculated by $\frac{S_{rbf}}{S_{rbf}+F_{rbf}}$, where S_{rbf} refers to the number of successful runs for which a better design is found, and F_{rbf} refers to the opposite condition. In each iteration, a random number is generated; if it is smaller than the success rate, the RBF-assisted local optimization will be carried out. The initial rate is set to 0.5. Within a learning period L, the initial rate is used, and then it is replaced by the real success rate. This is the way of judging whether local optimization should be used or not (Step 2 of TR-SADEA).

D. Parameter Settings

In TR-SADEA, the number of training data points to be used in the self-adaptive GP modeling and the RBF-assisted local search, as well as the learning period L need to be decided. For the first two, $4\times d$ and $10\times d$ are determined based on common empirical setting rules in surrogate model-assisted evolutionary algorithm research [22], [37] and antenna design optimization practice [5], [15]: the first one is often the least to maintain a GP model quality and the latter is often considered as sufficient to obtain a high-quality surrogate model. They are fixed in TR-SADEA and do not need the user to alter. Empirically, L is suggested to be within $[30, 50]$. It is clear that L is not sensitive. 50 is used in the following experiments.

In terms of parameters in DE operators, $F = 0.8, CR = 0.8$ are used in standard SADEA [5], which is also applicable to TR-SADEA. For the population size m, a new suggestion is that m should be around $2.5 \times d$. Too large m will cause slow convergence (i.e., more GP modeling and EM simulations, which are critical for complex antennas) and too small m may cause insufficient population diversity and fail the optimization. The above setting of m is based on an empirical study using various complex antennas.

IV. Experimental Results and Verifications

In this section, two real-world challenging base station antennas are used to demonstrate the TR-SADEA method. The first example is a 2G to 5G indoor base station antenna (5G-IBSA) [23] with 45 design variables and 12 specifications. The radiation pattern for indoor base station antennas is not strictly required for the optimal broadside radiation, but the antenna should be of relatively low profile (compact size) and low-cost. The 5G-IBSA will be designed to cover the existing 2G/3G/4G bands of 0.69 GHz to 0.96 GHz and 1.71 GHz to 2.7 GHz, as well as the desired 5G bands of 3.3 GHz to 3.8 GHz and 4.8 GHz to 5 GHz. The antenna will exhibit unidirectional radiation patterns with a realized gain of ≥ 5 dBi over the entire band. Note that in [23], a similar antenna is difficult to be directly optimized by the SADEA series because of the too long GP modeling time. Therefore, the design optimization process is divided into two stages to reduce the number of design variables and ad-hoc design knowledge is used. Although succeeds, the design parameter reduction method in [23] is only for this design case and is not applicable to other cases.

The second example is a 5G outdoor base station antenna (5G-OBSA) with 23 design variables and 18 specifications. The 5G-OBSA only covers 3.3 GHz to 5 GHz for 5G communications, but it is also proposed for dual-linear polarization (dual LP) base station antenna arrays, which are different

from the aforementioned indoor single antenna element. The particular challenge for this design is that the antenna needs to maintain a stable broadside radiation pattern, beamwidth, efficiency, and realized gain over the frequency band of interest. Importantly, the two-port isolation for the dual LP design will be taken into account. Again, the antenna size and overall dimension are critical to determining the practicability of this design in real-world applications that may require MIMO and smart-beam performance [20].

More details on the 5G-IBSA and 5G-OBSA are provided in the next subsections. Because no reasonably good initial designs can be provided, the search ranges provided by the designers for optimization are relatively wide. The 5G-IBSA and 5G-OBSA are optimized on a workstation with Intel 8-core i7 5960x 3GHz CPU, 64 GB RAM and 16 GB NVIDIA Quadro GP100 GPU. To further improve the efficiency of surrogate model training, 15 workers are used in parallel in Step 6 of the TR-SADEA framework (Section III (A)). The time consumptions recorded are wall clock time. The parameter settings of TR-SADEA are as discussed in section III (D).

To verify the optimization ability of TR-SADEA and the saved surrogate model training time by the proposed self-adaptive GP modeling method, four independent runs are carried out for the 5G-IBSA and 5G-OBSA. 10 runs or more, which are often used to draw statistical conclusions, are not affordable because a single run (with EM models having moderate mesh densities to ensure the accuracy and reliability of simulation results) for the 5G-IBSA and 5G-OBSA costs 1-2 weeks. Very often, this is the case for most complex antennas according to our experiments. However, to show the robustness and the effect of the RBF-assisted local optimization, statistical analysis and comparisons are still needed. Hence, a not complex antenna used by several antenna design optimization studies [16], [38] is employed, and 10 independent runs are carried out to infer the above properties for TR-SADEA.

A. Example 1: A Multi-wideband Indoor Base Station Antenna for 2G-5G Communications

The layout of the 45-variable 5G-IBSA is shown in Fig. 4. It consists of four layers, four bent metal strips and a reflector base. The metal strips in the first layer are used to introduce the resonant frequency and increase the bandwidth for the lower frequency band through coupling. The driven element of the 5G-IBSA, a dipole antenna and its stepped impedance feeding structure are in the second and third layers. The fourth layer introduces the resonant frequency for the higher frequency band. The rectangular reflector which forms the reflector base is used to ensure a good radiation pattern. The 5G-IBSA is fed by a 50Ω coaxial cable connected to the second and third layers and it is mainly made of copper with a thickness ranging from 0.8 mm to 1.2 mm across all the layers and components.

The 5G-IBSA is modeled and discretized in Computer Simulation Technology - Microwave Studio (CST-MWS) using a mesh density of 12 cells per wavelength to have about 5,200,000 mesh cells in total. Each EM simulation costs about

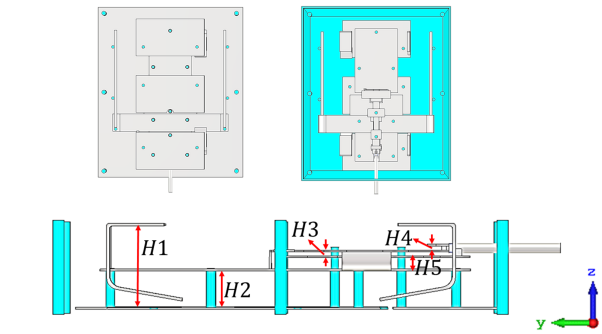

(a) Geometry.

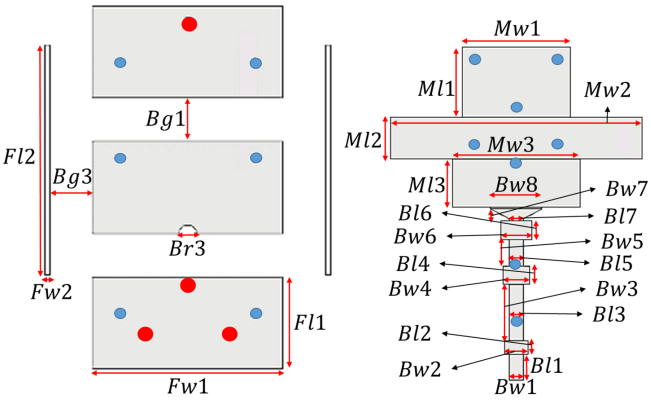

(b) First and second layers.

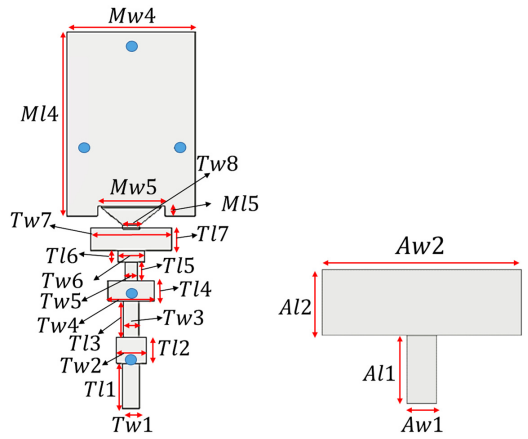

(c) Third and fourth layers.

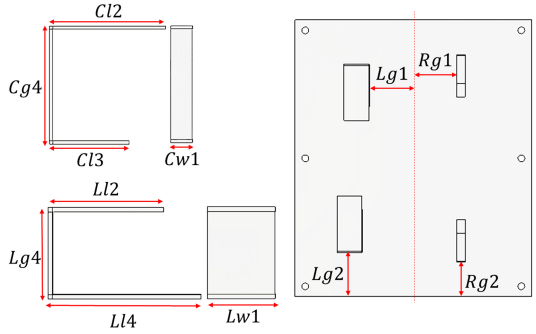

(d) Metal strips and reflector base.

Figure 4. Layout of the 2G/3G/4G/5G indoor base station antenna (5G-IBSA).

11 to 12 minutes on average. For the optimization of the 5G-IBSA, the 45 variables described in Fig. 4 and their given

Table I
SEARCH RANGES OF THE DESIGN VARIABLES AND THE OPTIMAL DESIGN BY TR-SADEA (ALL SIZES IN MM) (EXAMPLE 1)

N^o	$Variables$	Lower bound	Upper bound	TR-SADEA Optimum
1	$Tw1$	7.00	10.00	7.19
2	$Tl1$	16.00	19.00	18.67
3	$Tw2$	11.00	13.00	11.37
4	$Tl2$	9.00	12.00	11.26
5	$Tw3$	5.00	8.00	6.76
6	$Tl3$	14.00	16.00	14.64
7	$Tw4$	18.00	21.00	19.70
8	$Tl4$	7.00	10.00	9.14
9	$Tw5$	5.00	8.00	5.80
10	$Tl5$	7.00	10.00	8.42
11	$Tw6$	11.00	14.00	11.09
12	$Tl6$	2.00	5.00	3.74
13	$Tw7$	32.00	35.00	32.56
14	$Tl7$	7.00	10.00	9.59
15	$Aw1$	0.5	3.00	1.93
16	$Al1$	3.00	6.00	4.77
17	$Aw2$	9.00	13.00	12.21
18	$Al2$	2.00	5.00	4.71
19	$Mw1$	45.00	55.00	53.53
20	$Mw2$	90.00	100.00	96.82
21	$Mw3$	60.00	70.00	66.47
22	$Ml1$	30.00	35.00	33.94
23	$Ml2$	18.00	22.00	20.48
24	$Ml3$	22.00	26.00	23.67
25	$Mw4$	45.00	55.00	51.73
26	$Ml4$	70.00	80.00	71.13
27	$Bw1$	70.00	90.00	87.61
28	$Bl1$	33.50	50.00	39.61
29	$Bg1$	13.00	33.00	24.57
30	$Bg2$	39.00	59.00	45.33
31	$Bg3$	12.50	33.00	18.16
32	$Bl2$	104.00	124.00	111.38
33	$Bw2$	1.00	10.00	5.34
34	$Rg1$	27.80	47.80	30.98
35	$Rw1$	1.00	10.00	7.71
36	$Rg2$	7.50	27.50	18.54
37	$Rl2$	14.00	34.00	19.42
38	$Rg4$	4.00	17.00	4.45
39	$Rl3$	18.00	28.00	22.30
40	$Lg1$	30.00	40.00	33.38
41	$Lw1$	3.80	25.00	22.40
42	$Lg2$	7.50	27.50	12.18
43	$Ll2$	14.00	34.00	31.99
44	$Ll4$	22.00	42.00	39.46
45	$Lg4$	4.00	15.00	12.83

search ranges in Table I are considered. The optimization goal is the minimization of the fitness function, F_{IBSA} in (13), to satisfy the design specifications in Table II. When all the design specifications in Table II are satisfied, F_{IBSA} is equal to zero.

$$F_{IBSA} = \sum_{i=1}^{4} \{w_1 \times max([S_{11}^i + 10dB, 0]) + ... \\ w_2 \times max([5dBi - G^i, 0]) + w_2 \times max([1 - NR^i, 0])\} \quad (13)$$

where i is the index for the current frequency band out of the four frequency bands for the quad-band operations of the 5G-IBSA. The use of NR (number of resonance) is because whether the S-parameter requirements in the required cellular bands can be met is not known before the optimization. Hence, matching networks might be needed and resonance

Table II
DESIGN SPECIFICATIONS AND THE PERFORMANCE OF AN OPTIMAL DESIGN (EXAMPLE 1)

N^o	Item	Specification	TR-SADEA Optimum
1	Maximum Reflection Coefficient (S_{11}) (0.69 to 0.96 GHz)	$\leq$ -10 dB	-10.64 dB
2	Maximum Reflection Coefficient (S_{11}) (1.71 to 2.70 GHz)	$\leq$ -10 dB	-10.03 dB
3	Maximum Reflection Coefficient (S_{11}) (3.30 to 3.80 GHz)	$\leq$ -10 dB	-10.81 dB
4	Maximum Reflection Coefficient (S_{11}) (4.80 to 5.00 GHz)	$\leq$ -10 dB	-11.51 dB
5	Minimum Realized Gain (G) (0.69 to 0.96 GHz)	$\geq$ 5 dBi	5.88 dBi
6	Minimum Realized Gain (G) (1.71 to 2.70 GHz)	$\geq$ 5 dBi	6.57 dBi
7	Minimum Realized Gain (G) (3.30 to 3.80 GHz)	$\geq$ 5 dBi	7.80 dBi
8	Minimum Realized Gain (G) (4.80 to 5.00 GHz)	$\geq$ 5 dBi	6.04 dBi
9	Number of Resonance (NR) (0.69 - 0.96 GHz) (if S_{11} > -10 dB)	≥ 1	Defaulted to 1
10	Number of Resonance (NR) (1.71 - 2.71 GHz) (if S_{11} > -10 dB)	≥ 1	Defaulted to 1
11	Number of Resonance (NR) (3.30 - 3.80 GHz) (if S_{11} > -10 dB)	≥ 1	Defaulted to 1
12	Number of Resonance (NR) (4.80 - 5.00 GHz) (if S_{11} > -10 dB)	≥ 1	Defaulted to 1

is essential for building a matching network. w_1 and w_2 are the penalty coefficients. w_1 is set to 1 and w_2 is set to 50. Using these penalty coefficients: The optimization procedure preferentially ensures that the specifications for G^i and NR^i are satisfied first by largely penalizing F_{IBSA} if they are violated. Then, meeting the S_{11}^i requirement becomes the primary focus of the optimization procedure as soon as G^i and NR^i are satisfied. Note that resonances are only required in the antenna's operating bands when the return loss cannot meet the specification. Hence, if $S_{11}^i \leq -10dB$ in (13) (or $VSWR \leq 2$), the resonance is no longer obligatory in the i^{th} frequency band due to good matching (low mismatch loss) and NR^i is defaulted to 1.

All four TR-SADEA runs for the 5G-IBSA obtain designs that satisfy all the desired specifications in Table II using 1890 EM simulations (17.2 days) on average. From a practical design viewpoint, a maximum in-band reflection coefficient less than or equal to -9.5 dB and a minimum in-band realized gain greater than or equal to 4.5 dBi are satisfactory for the 5G-IBSA. Using this design criterion, all four TR-SADEA runs for the 5G-IBSA obtain satisfactory designs using 1579 EM simulations (14 days) on average. Considering the 45 design variables, 12 specifications and very complex structure, TR-SADEA still obtains satisfactory results in a practical time.

Regarding the training cost in the optimization process, a total number of 186,561 surrogate models (60.4 hours, 15 workers in parallel) are trained in TR-SADEA on average compared to the expected 2,548,800 surrogate models (calculated by $N_{specs} \times N_{pop} \times N_{it}$, see Section I) on average, if the proposed self-adaptive GP modeling is not used (i.e., the GP modeling method in standard SADEA). This shows that the self-adaptive GP modeling in TR-SADEA reduces on average almost 93% of the GP modeling time for standard

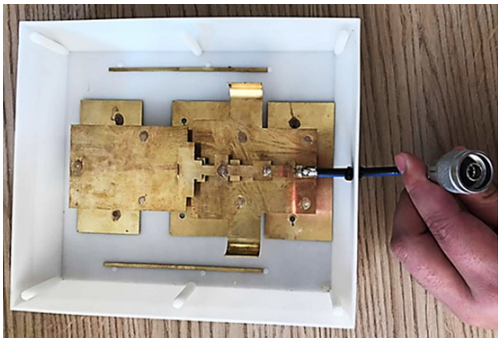

(a) Fabricated prototype.

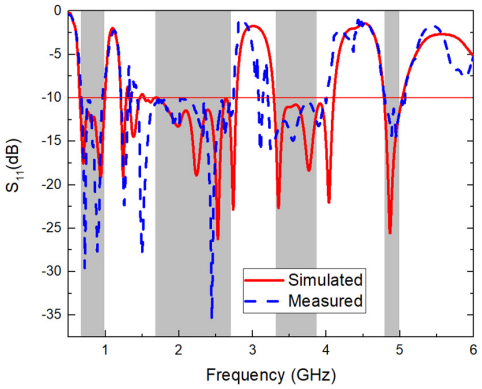

(b) Return loss (S_{11}).

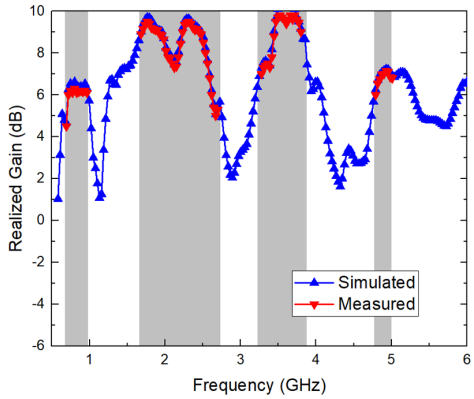

(c) Realized gain.

Figure 5. Physical implementation and measurement results of the TR-SADEA optimized 5G-IBSA.

SADEA for this example. The saved time is about 32 days on average using 15 parallel workers in the workstation. It can be inferred that when the number of design variables or specifications increases or the computer cannot afford many parallel workers, standard SADEA may cost enormous time for complex antennas. Note that in the above estimation, it is assumed that TR-SADEA and standard SADEA use the same average number of iterations with the same population size. This favors standard SADEA due to neglecting the convergence speed improvement of TR-SADEA, which will be detailed in Section IV (D).

One of the obtained optimal designs is shown in Table I. The performance of this design is shown in Table II and it is fabricated. The fabricated 5G-IBSA is shown in Fig. 5(a) and the size is 170.6 mm $\times$ 200 mm $\times$ 37 mm. It can be seen that the antenna is compact, which is $0.39\lambda_0 \times 0.46\lambda_0 \times 0.09\lambda_0$, where λ_0 is the free-space wavelength at 690 MHz. The simulation and measurement results for the return loss and realized gain across all the bands of interest are shown in Fig. 5(b) and Fig. 5(c). From Fig. 5(b) and Fig. 5(c), it can be seen that the simulation results are generally in close agreement with the measurement results. It is further observed that the low-frequency band (< 2.7 GHz) measurement result is well aligned with the simulation result, while some slight difference can be observed for S_{11} over 3.3 - 3.7 GHz. This is because the high-frequency radiating elements are determined by the stepped impedance feeding structure at the antenna feed, which can be easily affected by the soldering to the cable and SMA connector.

To consider fabrication tolerance, which is ± 0.1 mm for the used fabrication process, a Monte-Carlo analysis is carried out. For each of the 45 parameters of the design that is used for fabrication, a uniformly distributed random noise within ± 0.1 mm is added and 200 samples are used. Simulation results show that all 200 samples meet the desired performance specifications in Table II.

B. Example 2: A Wideband Antenna with Stable Radiation for 5G Outdoor Base Stations

The layout of the 23-variable 5G-OBSA is shown in Fig. 6. It consists of three parts: double-oval shaped dipoles, Γ-shaped feeding lines and a reflector base. The double-oval shaped dipoles and the Γ-shaped feeding lines are implemented on an FR4 substrate with a thickness of 0.8 mm, a relative

Table III
SEARCH RANGES OF THE DESIGN VARIABLES AND THE OPTIMAL DESIGN BY TR-SADEA (ALL SIZES IN MM) (EXAMPLE 2)

Nº	$Variables$	Lower bound	Upper bound	TR-SADEA Optimum
1	$lf1$	1.00	10.00	1.95
2	$lf2$	1.00	10.00	1.71
3	$lf3$	1.00	10.00	3.00
4	$lf4$	0.10	1.50	0.14
5	$lf5$	0.10	1.50	0.22
6	$lf6$	0.10	15.00	4.61
7	$wf2$	0.10	1.50	0.97
8	$wf3$	0.10	1.50	0.35
9	$wf4$	0.10	5.00	2.27
10	$wf5$	0.10	5.00	2.53
11	$wf6$	0.10	1.50	0.52
12	gw	0.10	1.50	0.63
13	ls	16.00	30.00	16.32
14	$x1$	7.50	15.00	12.04
15	$b1$	3.00	5.00	4.69
16	$t1$	0.50	3.00	2.58
17	$x2$	3.00	8.00	5.54
18	$b2$	0.50	3.00	2.02
19	$t2$	0.20	0.80	0.61
20	$g1$	1.00	3.00	1.94
21	$g2$	1.00	3.00	2.58
22	wg	5.00	15.00	6.74
23	rw	60.00	85.00	84.45

permittivity of 4.4 and a loss tangent of 0.02. The crossed-dipole arms are placed along the diagonal of the substrate to ensure a $\pm 45^{\circ}$ polarization and each arm has an inner oval-shaped loop and an outer oval-shaped loop. Each feeding structure has a frontal Γ-shaped feeding line and two rear rectangular patches which are connected to both the crossed-dipole and the reflector base. The double-oval shaped dipoles and the Γ-shaped feeding lines are well matched and provide a wide impedance bandwidth. The reflector base is used to achieve a better unidirectional radiation pattern.

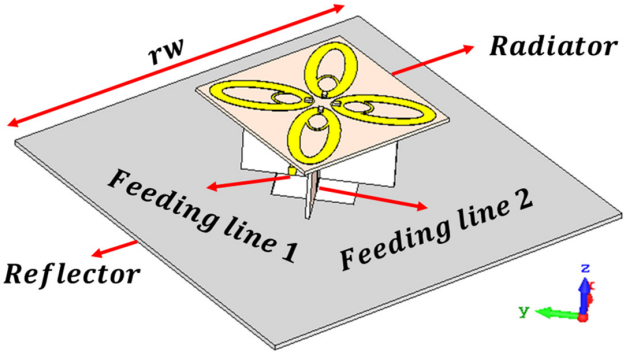

(a) Geometry

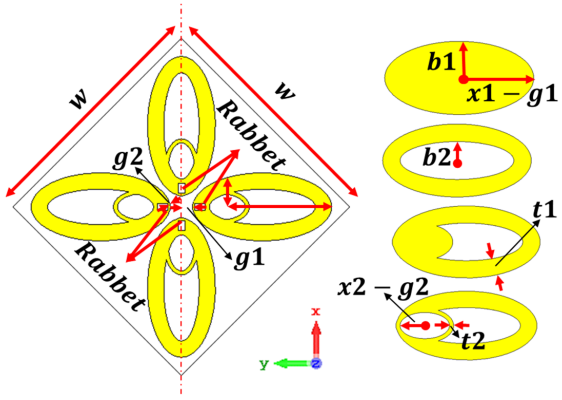

(b) Crossed-dipole radiator.

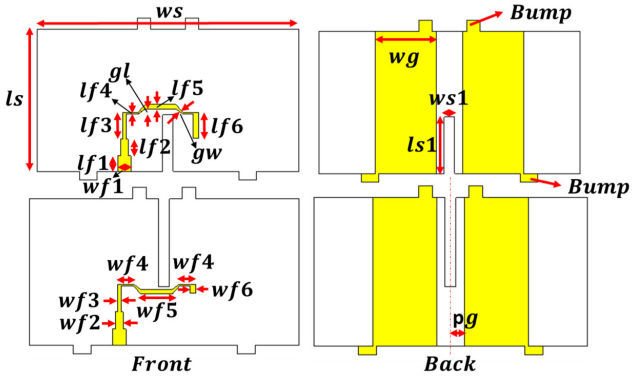

(c) Front and back views of two feeding structures.

Figure 6. Layout of the 5G outdoor base station antenna (5G-OBSA).

The 5G-OBSA is modeled and discretized in CST-MWS using a mesh density of 15 cells per wavelength to have about 2,630,000 mesh cells in total. Each EM simulation costs about 9 to 10 minutes on average. For the optimization of the 5G-OBSA, the 23 variables described in Fig. 6 and their given search ranges in Table III are considered. The optimization goal is the minimization of the fitness function, F_{OBSA} in (14), to satisfy the design specifications in Table IV. When all the design specifications in Table III are satisfied, F_{OBSA} is equal to zero.

Table IV
DESIGN SPECIFICATIONS AND THE PERFORMANCE OF AN OPTIMAL DESIGN (EXAMPLE 2)

N^{o}	Item	Specification	TR-SADEA Optimum
1	Maximum Reflection Coefficient (S_{11}) (3.3 to 3.8 GHz)	$\leq$ -10 dB	-12.04 dB
2	Maximum Reflection Coefficient (S_{11}) (4.8 to 5.0 GHz)	$\leq$ -10 dB	-12.41 dB
3	Maximum Reflection Coefficient (S_{22}) (3.3 to 3.8 GHz)	$\leq$ -10 dB	-11.68 dB
4	Maximum Reflection Coefficient (S_{22}) (4.8 to 5.0 GHz)	$\leq$ -10 dB	-12.19 dB
5	Maximum Transmission Coefficient (S_{12}) (3.3 to 3.8 GHz)	$\leq$ -20 dB	-24.55 dB
6	Maximum Transmission Coefficient (S_{12}) (4.8 to 5.0 GHz)	$\leq$ -20 dB	-36.35 dB
7	Minimum Realized Gain (G) (3.3 to 3.8 GHz)	$\geq$ 5 dBi	8.00 dBi
8	Minimum Realized Gain (G) (4.8 to 5.0 GHz)	$\geq$ 5 dBi	7.87 dBi
9	Minimum Front-to-Back Ratio (FBR) (3.3 to 3.8 GHz)	$\geq$ 15 dB	15.89 dB
10	Minimum Front-to-Back Ratio (FBR) (4.8 to 5.0 GHz)	$\geq$ 15 dB	15.51 dB
11	Minimum Half-power Beamwidth ($HPBW_l$) (3.3 to 3.8 GHz)	$\geq 60^{\circ}$	68.68°
12	Maximum Half-power Beamwidth ($HPBW_u$) (3.3 to 3.8 GHz)	$\leq 70^{\circ}$	69.81°
13	Minimum Half-power Beamwidth ($HPBW_l$) (4.8 to 5.0 GHz)	$\geq 60^{\circ}$	66.13°
14	Maximum Half-power Beamwidth ($HPBW_u$) (4.8 to 5.0 GHz)	$\leq 70^{\circ}$	69.27°
15	Number of Resonance (NR_1) (3.3 to 3.8 GHz) (if S_{11} > -10 dB)	≥ 1	Defaulted to 1
16	Number of Resonance (NR_1) (4.8 to 5.0 GHz) (if S_{11} > -10 dB)	≥ 1	Defaulted to 1
17	Number of Resonance (NR_2) (3.3 to 3.8 GHz) (if S_{22} > -10 dB)	≥ 1	Defaulted to 1
18	Number of Resonance (NR_2) (4.8 to 5.0 GHz) (if S_{22} > -10 dB)	≥ 1	Defaulted to 1

$$
\begin{aligned}
F_{OBSA} = \sum_{i=1}^{2} \Big\{ & w_1 \times \big[max([S_{11}^i + 10\,dB, 0]) + ... \\
& max([S_{22}^i + 10\,dB, 0]) + max([S_{12}^i + 20\,dB, 0]) \big] + ... \\
& w_2 \times \big[max([5\,dBi - G^i, 0]) + max([15\,dB - FBR^i, 0]) + ... \\
& max([60^{\circ} - HPBW_l^i, 0]) + max([HPBW_u^i - 70^{\circ}, 0]) + ... \\
& max([1 - NR_1^i, 0]) + max([1 - NR_2^i, 0]) \big] \Big\}
\end{aligned} \tag{14}
$$

where i is the index for the current frequency band out of the two frequency bands for the dual-band operations of the 5G-OBSA, and w_1 and w_2 are the penalty coefficients. w_1 is set to 1 and w_2 is set to 50. The reason for setting w_1 and w_2 is the same as example 1. NR_1^i and NR_2^i are also be defaulted to 1 subject to the same conditions and reasons given for example 1 (i.e., if $S_{11}^i \leq -10dB$ and $S_{22}^i \leq -10dB$ in (14) for NR_1^i and NR_2^i, respectively).

All four TR-SADEA runs for the 5G-OBSA obtain designs that satisfy all the desired specifications in Table IV using 1708 EM simulations (11.9 days) on average. The satisfactory speci-

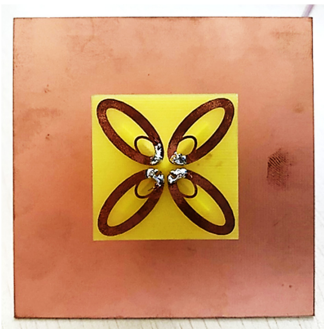

(a) Fabricated prototype.

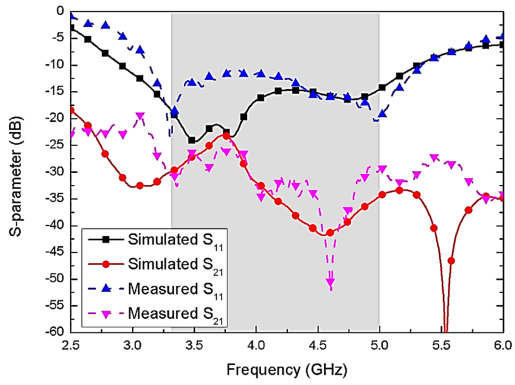

(b) Return loss (S_{11}).

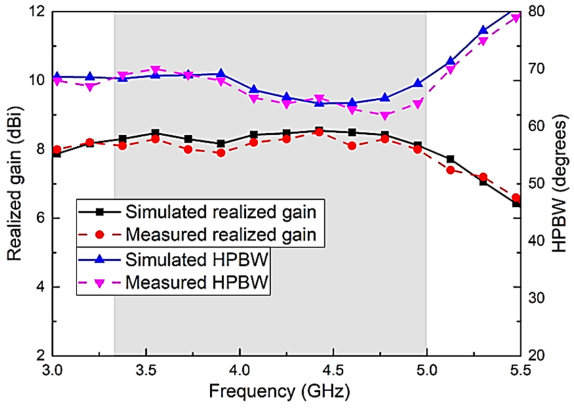

(c) Realized gain and half-power beamwidth.

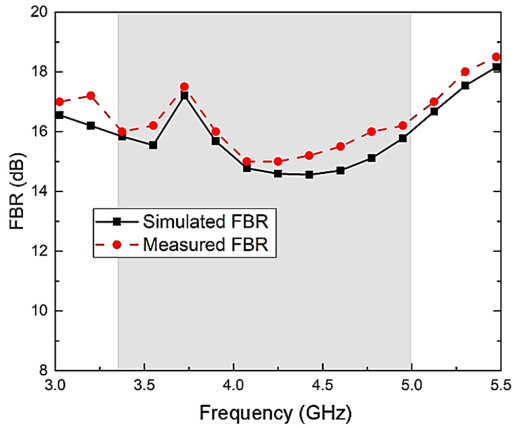

(d) Front-to-back ratio.

Figure 7. Physical implementation and measurement results of the TR-SADEA optimized 5G-OBSA.

fications for the in-band reflection coefficient and realized gain for the 5G-OBSA are the same as example 1. Additionally, the maximum in band coupling coefficients less than or equal to -15 dB, minimum in-band half power beamwidths greater than or equal to $55°$, and maximum in-band half power beamwidths less than or equal to $75°$ are also considered satisfactory for the 5G-OBSA from a practical design viewpoint. Using this design criterion, all four TR-SADEA runs obtain satisfactory designs using 1144 EM simulations (7.6 days) on average. Hence, the optimization ability and efficiency of TR-SADEA are demonstrated.

Regarding the training cost in the optimization process, a total number of 165,132 surrogate models (21.4 hours, 15 workers in parallel) are trained in TR-SADEA on average compared to the expected 1,779,840 surrogate models (calculated by $N_{specs} \times N_{pop} \times N_{it}$, see Section I) on average, if the proposed self-adaptive GP modeling is not used (i.e., the GP modeling method in standard SADEA). This shows that the self-adaptive GP modeling in TR-SADEA reduces almost 94% of the GP modeling time on average for standard SADEA for this example. The saved time is about 9 days on average using 15 parallel workers in the workstation. Like example 1, this estimation favors standard SADEA due to neglecting the convergence speed improvement of TR-SADEA.

One of the obtained optimal designs is shown in Table III. The performance of this design is shown in Table IV and it is fabricated. The fabricated 5G-OBSA is shown in Fig. 7(a) and the size is 84.3 mm $\times$ 84.3 mm $\times$ 18.1 mm. It can be seen that the antenna is compact, which is $0.93\lambda_0 \times 0.93\lambda_0 \times 0.20\lambda_0$, where λ_0 is the free-space wavelength at 3.3 GHz. The simulation and measurement results for the return loss, realized gain, half-power beamwidth, and front-to-back ratio across all the bands of interest are shown in Fig. 7(b), Fig. 7(c) and Fig. 7(d). From Fig. 7(b), Fig. 7(c) and Fig. 7(d), the S_{11} and antenna gain are in reasonably good agreement between the simulated and measured results over the entire frequency band of interest at 3.3 - 5.0 GHz. A slight difference can be seen from S11 at around 3.5 GHz. It is likely due to the fabrication errors of the soldering, which has an impact on the low frequency radiating element (outer elliptical ring). This can be improved by using high precision soldering machines. Even though, the overall S_{11} of the outdoor antenna prototype is all below -10 dB over the desired band.

To account for fabrication tolerance, the tolerance value is also ± 0.1 mm. The same procedure used for example 1 is applied using the fabricated design. In the 200 samples, except one maximum half-power beamwidth specification is around $71°$ compared with the desired specification of $70°$, all other performances meet the desired specifications in Table IV.

C. Comparisons with Existing Antenna Design Optimization Methods

To the best of our knowledge, there is currently no published antenna design optimization method handling design cases with many design variables (e.g., more than 30) and specifications (e.g., more than 10) for TR-SADEA to be compared with statistically. Even though, typical existing antenna design

optimization methods are used. The computing budget is two weeks using the same work station except that the optimization method converges before two weeks.

Regarding local optimization-based methods, it is shown that the performance highly depends on how good the starting point (initial design) is [13]. As said above, due to the many design variables and specifications involved, a good initial design cannot be obtained for the 5G-IBSA and the 5G-OBSA. Five starting points by Latin Hypercube Sampling [33] of the design space are tried using the trust-region method [39] for both cases. However, local optimal solutions far from the specifications are obtained using all of the starting points.

Regarding standard global optimization methods, one DE run and one PSO run are carried out. After two weeks' optimization, the best designs obtained by DE and PSO for both examples are still far from the specifications. This is not a surprise because as said in Section I, the SADEA series can obtain better design quality using less than 10% of EM simulations compared to DE and PSO [5], [13], [15], [16]. Hence, DE and PSO are not affordable to address the two base station antennas only considering the number of necessary EM simulations to obtain the optimal design.

A standard SADEA run is then carried out and the optimization time is two weeks. For the 5G-IBSA, the current best result is max(S_{11}) of -5.1 dB, -11.4 dB, -4.8 dB, and -10.7 dB in the respective bands, which is far from satisfactory although other specifications are satisfied. For the 5G-OBSA, even removing the most challenging front-to-back-ratio specification, the current best result is max(S_{11}) of -6.1 dB and -11.0 dB in the respective bands, max(S_{22}) of -5.1 dB and -6.0 dB in the respective bands, and max(S_{12}) of -21.8 dB and -9.7 dB in the respective bands, although other specifications are satisfied. As said above, the GP modeling costs a very long time making them not able to optimize 5G base station antennas with many design variables and specifications efficiently, although they are expected to succeed after a longer optimization time.

Note that SADEA-II [14] and PSADEA [15], [16] are not suitable candidates for comparison. SADEA-II focuses on the method to handle the discrepancy between multi-fidelity EM models while TR-SADEA considers a single-fidelity EM model and is compatible with SADEA-II. PSADEA obtains higher quality antenna designs with fewer EM simulations at the cost of a larger number of GP modeling, which is not fit for the targeted problem.

Recently, a novel method is proposed. Instead of mapping design parameters to antenna performances, the response (e.g., S_{11} over all interested frequencies) is mapped with the design parameters and the specifications are then extracted from the response [40], [41]. The challenge for this kind of method is the so-called "curse of dimensionality" (e.g., it has many design variables or the search range is wide) [40], [41]. Hence, methods based on this idea are not fit for the targeted problem. However, they provide an accurate surrogate model of the antenna around a reasonable initial design, which is useful for antenna circuit co-design, while the SADEA series does not.

Table V
RANGES OF THE DESIGN VARIABLES (ALL SIZES IN MM) FOR THE HYBRID DRA

$Variables$	a_x	a_y	a_z	a_c	u_s	w_s	y_s
Lower bound	6	12	6	6	0.5	4	2
Upper bound	10	16	10	8	4	12	12

Table VI
STATISTICS OF THE BEST OBJECTIVE FUNCTION VALUES (MAX.(S_{11})) USING DIFFERENT METHODS (HYBRID DRA PROBLEM) (OVER 10 RUNS)

$Method$	$Best$	$Worst$	$Mean$	$Median$	$Std.$
TR-SADEA	-25.48 dB	-22.57 dB	-23.98 dB	-24.09 dB	0.92
SADEA-AGP	-24.98 dB	-22.61 dB	-23.87 dB	-23.95 dB	0.73
SADEA	-25.46 dB	-22.71 dB	-23.96 dB	-23.76 dB	1.0438

D. Verification of TR-SADEA Operators

Besides the above verifications of TR-SADEA, there are still three interesting questions: (1) The standard SADEA has a high robustness [5], [13]. Does this apply to TR-SADEA? (2) Compared to standard SADEA, does the self-adaptive GP modeling (Section III (B)) sacrifice the performance? (3) To what extent does the RBF-assisted local optimization (Section III (C)) help the design optimization? To answer those questions, statistical analysis and comparisons (e.g., over 10 runs) are unavoidable. However, due to the computational cost, it is not affordable to use the above complex antennas for this study. An alternative is to use mathematical benchmark problems, but we found that many popular optimization algorithms that are successful for mathematical benchmark problems cannot succeed for antenna design optimization. Hence, a computationally cheap hybrid dielectric resonator antenna (DRA) [38], [13] is optimized for 10 times as a reasonable approximation to infer the analysis result of using complex antennas.

More details on the hybrid DRA problem can be found in [38], [13]. For the design exploration, the objective function is stated in (15) and the search ranges of the design variables are shown in Table V. For comparisons, the performance of TR-SADEA is compared with SADEA (using $4 \times$ d training data points) and SADEA-AGP (using $4 \times$ d training data points, self-adaptive GP modeling but without RBF-assisted local optimization). To make all the methods converge, the computing budget is 1000 EM simulations over 10 independent runs. The algorithmic parameter settings are as previously discussed; however, m is set to $4 \times d$ because of the hybrid DRA's very narrow optimal region [13], [15] which makes it distinct from other antennas.

$$\text{minimize} \quad max|S_{11}| \quad 5.28\,GHz - 5.72\,GHz \tag{15}$$

The statistics (over 10 independent runs) are shown in Table VI. In terms of solution quality, the following observations can be made: (1) In all the 10 runs, TR-SADEA obtains highly satisfactory results even in the worst case. (2) TR-SADEA shows good robustness as the standard deviation is low. (3)

The design solution quality of TR-SADEA is very similar to SADEA-AGP and SADEA. In other words, the self-adaptive GP modeling method does not diminish the optimization quality.

In terms of efficiency, a -20 dB reference value for $\max(S_{11})$ in the operational band of the hybrid DRA problem as suggested in [13] is used for the evaluation of all methods. TR-SADEA, SADEA-AGP and SADEA use 368, 466, and 452 EM simulations on the average, respectively, to obtain an average maximum (S_{11}) of -20 dB. This shows that more than 20% of the iterations (i.e., EM simulations and GP modelings) are saved by TR-SADEA. This validates the added efficiency improvement of the RBF-assisted local optimization in TR-SADEA.

V. Conclusions

In this paper, the TR-SADEA method has been proposed. The effectiveness and efficiency of TR-SADEA are demonstrated by the simulation and measurement results of two real-world complex antennas with challenging performance requirements, for which, there is no known efficient method to optimize them to the best of our knowledge. Thanks to the self-adaptive GP modeling method, the very long surrogate model training time can be saved by more than 90%, and the total optimization time, therefore, becomes acceptable. Thanks to the RBF-assisted local optimization method and the new surrogate model-assisted optimization framework making use of it, the convergence speed is further improved (reducing 20% GP modeling and EM simulations by inference). To the best of our knowledge, TR-SADEA is the first efficient method to optimize such complex antennas with many design variables and specifications. Future works will include behavioral analysis of TR-SADEA and its improvement.

References

[1] A. Bekasiewicz, S. Koziel, and Q. S. Cheng, "Reduced-cost constrained miniaturization of wideband antennas using improved trust-region gradient search with repair step," *IEEE Antennas and Wireless Propagation Letters*, vol. 17, no. 4, pp. 559–562, 2018.

[2] S. Koziel, J. W. Bandler, and Q. S. Cheng, "Robust trust-region space-mapping algorithms for microwave design optimization," *IEEE Transactions on Microwave Theory and Techniques*, vol. 58, no. 8, pp. 2166–2174, 2010.

[3] N. Jin and Y. Rahmat-Samii, "Advances in particle swarm optimization for antenna designs: real-number, binary, single-objective and multiobjective implementations," *IEEE transactions on antennas and propagation*, vol. 55, no. 3, pp. 556–567, 2007.

[4] Y. Sato, F. Campelo, and H. Igarashi, "Meander line antenna design using an adaptive genetic algorithm," *IEEE Transactions on Magnetics*, vol. 49, no. 5, pp. 1889–1892, 2013.

[5] B. Liu *et al.*, "An efficient method for antenna design optimization based on evolutionary computation and machine learning techniques," *IEEE Trans. on Antennas and Propagation*, vol. 62, no. 1, pp. 7–18, 2014.

[6] P. Rocca, G. Oliveri, and A. Massa, "Differential evolution as applied to electromagnetics," *IEEE Antennas and Propagation Magazine*, vol. 53, no. 1, pp. 38–49, 2011.

[7] Z. D. Zaharis and T. V. Yioultsis, "A novel adaptive beamforming technique applied on linear antenna arrays using adaptive mutated boolean pso," *Progress In Electromagnetics Research*, vol. 117, pp. 165–179, 2011.

[8] R. Storn and K. Price, "Differential evolution–a simple and efficient heuristic for global optimization over continuous spaces," *Journal of Global Optimization*, vol. 11, no. 4, pp. 341–359, 1997.

[9] J. Kennedy, "Particle swarm optimization," *Encyclopedia of machine learning*, pp. 760–766, 2010.

[10] S. Koziel and S. Ogurtsov, *Antenna design by simulation-driven optimization*. Springer, 2014.

[11] I. Couckuyt, F. Declercq, T. Dhaene, H. Rogier, and L. Knockaert, "Surrogate-based infill optimization applied to electromagnetic problems," *International Journal of RF and Microwave Computer-Aided Engineering*, vol. 20, no. 5, pp. 492–501, 2010.

[12] Y. Jin, "Surrogate-assisted evolutionary computation: Recent advances and future challenges," *Swarm and Evolutionary Computation*, vol. 1, no. 2, pp. 61–70, 2011.

[13] V. Grout, M. O. Akinsolu, B. Liu, P. I. Lazaridis, K. K. Mistry, and Z. D. Zaharis, "Software solutions for antenna design exploration: A comparison of packages, tools, techniques, and algorithms for various design challenges," *IEEE Antennas and Propagation Magazine*, vol. 61, no. 3, pp. 48–59, 2019.

[14] B. Liu, S. Koziel, and N. Ali, "Sadea-ii: A generalized method for efficient global optimization of antenna design," *Journal of Computational Design and Engineering*, vol. 4, no. 2, pp. 86–97, 2017.

[15] M. O. Akinsolu, B. Liu, V. Grout, P. I. Lazaridis, M. E. Mognaschi, and P. Di Barba, "A parallel surrogate model assisted evolutionary algorithm for electromagnetic design optimization," *IEEE Transactions on Emerging Topics in Computational Intelligence*, vol. 3, no. 2, pp. 93–105, 2019.

[16] B. Liu, M. O. Akinsolu, N. Ali, and R. Abd-Alhameed, "Efficient global optimisation of microwave antennas based on a parallel surrogate model-assisted evolutionary algorithm," *IET Microwaves, Antennas & Propagation*, vol. 13, no. 2, pp. 149–155, 2018.

[17] L.-H. Wen, S. Gao, Q. Luo, C.-X. Mao, W. Hu, Y. Yin, Y. Zhou, and Q. Wang, "Compact dual-polarized shared-dipole antennas for base station applications," *IEEE Transactions on Antennas and Propagation*, vol. 66, no. 12, pp. 6826–6834, 2018.

[18] A. Elsakka, T. Bressner, A. van den Biggelaar, A. Al-Rawi, U. Johannsen, M. Ivashina, and A. Smolders, "On the use of focal-plane arrays in mm-wave 5g base stations," *12th European Conference on Antennas and Propagation (EuCAP)*, pp. 1–4, 2018.

[19] S. F. Jilani and A. Alomainy, "A multiband millimeter-wave 2-d array based on enhanced franklin antenna for 5g wireless systems," *IEEE Antennas and Wireless Propagation Letters*, vol. 16, pp. 2983–2986, 2017.

[20] W. Hong, Z. H. Jiang, C. Yu, J. Zhou, P. Chen, Z. Yu, H. Zhang, B. Yang, X. Pang, M. Jiang *et al.*, "Multibeam antenna technologies for 5g wireless communications," *IEEE Transactions on Antennas and Propagation*, vol. 65, no. 12, pp. 6231–6249, 2017.

[21] T. S. Rappaport, Y. Xing, G. R. MacCartney, A. F. Molisch, E. Mellios, and J. Zhang, "Overview of millimeter wave communications for fifth-generation (5g) wireless networks with a focus on propagation models," *IEEE Transactions on Antennas and Propagation*, vol. 65, no. 12, pp. 6213–6230, 2017.

[22] M. Emmerich, K. Giannakoglou, and B. Naujoks, "Single-and multiobjective evolutionary optimization assisted by Gaussian random field metamodels," *IEEE Transactions on Evolutionary Computation*, vol. 10, no. 4, pp. 421–439, 2006.

[23] Q. Hua, Y. Huang, C. Song, M. O. Akinsolu, B. Liu, T. Jia, Q. Xu, and A. Alieldin, "A novel compact quadruple-band indoor base station antenna for 2g/3g/4g/5g systems," *IEEE Access*, vol. 7, pp. 151 350–151 358, 2019.

[24] C. Rasmussen, "Gaussian processes in machine learning," *Advanced Lectures on Machine Learning*, pp. 63–71, 2004.

[25] T. J. Santner, B. J. Williams, and W. I. Notz, *The design and analysis of computer experiments*. Springer Science & Business Media, 2013.

[26] J. Dennis and V. Torczon, "Managing approximation models in optimization," *Multidisciplinary design optimization: State-of-the-art*, pp. 330–347, 1997.

[27] I. Couckuyt, A. Forrester, D. Gorissen, F. De Turck, and T. Dhaene, "Blind kriging: Implementation and performance analysis," *Advances in Engineering Software*, vol. 49, pp. 1–13, 2012.

[28] D. Guo, Y. Jin, J. Ding, and T. Chai, "Heterogeneous ensemble-based infill criterion for evolutionary multiobjective optimization of expensive problems," *IEEE transactions on cybernetics*, vol. 49, no. 3, pp. 1012–1025, 2018.

[29] B. Liu, Q. Zhang, and G. G. E. Gielen, "A gaussian process surrogate model assisted evolutionary algorith for medium scale expensive optimization problems," *IEEE Trans. on Evolutionary Computation*, vol. 18, no. 2, pp. 180–192, 2014.

[30] M. J. Powell, "The theory of radial basis function approximation in 1990," *Advances in numerical analysis*, pp. 105–210, 1992.

[31] R. G. Regis, "Evolutionary programming for high-dimensional constrained expensive black-box optimization using radial basis functions,"

IEEE Transactions on Evolutionary Computation, vol. 18, no. 3, pp. 326–347, 2013.

[32] D. J. Toal, N. W. Bressloff, and A. J. Keane, "Kriging hyperparameter tuning strategies," *AIAA journal*, vol. 46, no. 5, pp. 1240–1252, 2008.

[33] M. Stein, "Large sample properties of simulations using latin hypercube sampling," *Technometrics*, pp. 143–151, 1987.

[34] B. Liu, G. Gielen, and F. V. Fernández, "Automated design of analog and high-frequency circuits," in *A computational intelligence approach*. Springer, 2014.

[35] A. K. Jain, R. C. Dubes *et al.*, *Algorithms for clustering data*. Prentice hall Englewood Cliffs, NJ, 1988, vol. 6.

[36] P. T. Boggs and J. W. Tolle, "Sequential quadratic programming," *Acta numerica*, vol. 4, pp. 1–51, 1995.

[37] D. R. Jones *et al.*, "Efficient global optimization of expensive black-box functions," *Journal of Global Optimization*, vol. 13, no. 4, pp. 455–492, 1998.

[38] S. Koziel, S. Ogurtsov, I. Couckuyt, and T. Dhaene, "Cost-efficient electromagnetic-simulation-driven antenna design using co-kriging," *IET Microwaves, Antennas & Propagation*, vol. 6, no. 14, pp. 1521–1528, 2012.

[39] D. S. SE. (2019) Automatic Optimization cst studio suite. [Online]. Available: https://www.3ds.com/products-services/simulia/products/cst-studio-suite/optimization/

[40] L.-Y. Xiao, W. Shao, F.-L. Jin, and B.-Z. Wang, "Multiparameter modeling with ann for antenna design," *IEEE Transactions on Antennas and Propagation*, vol. 66, no. 7, pp. 3718–3723, 2018.

[41] Q. Wu, H. Wang, and W. Hong, "Multi-stage collaborative machine learning and its application to antenna modeling and optimization," *IEEE Transactions on Antennas and Propagation*, 2020.